Using Optical Imaging and Image Processing to Verify a Layer in a Laser Powder Bed Fusion Process

by

Maya Padmini Kota

Bachelor of Science in Mechanical Engineering
University of Southern California, 2021

Submitted to the Department of Mechanical Engineering
in Partial Fulfillment of the Requirements for the Degree of
MASTER OF ENGINEERING IN ADVANCED MANUFACTURING AND DESIGN
at the
MASSACHUSETTS INSTITUTE OF TECHNOLOGY
February 2023

Author.....
Maya Padmini Kota
Department of Mechanical Engineering
September 19, 2022

Certified by .....
David Hardt
Ralph E. and Eloise F. Cross Professor of Mechanical Engineering
Thesis Supervisor

Accepted by.....
Nicolas Hadjiconstantinou
Chairman, Department Committee on Graduate Theses

This page is intentionally left blank.

List of Figures and Tables

Abstract

Additive manufacturing (AM) allows for the creation of complex geometries that cannot be created with traditional manufacturing methods. AM is widely used in regulated industries such as medical and aerospace which require objective evidence of good manufacturing processes (GMP) for auditing purposes. Within AM, important powder layer characteristics must be met to ensure final part quality. Such properties are currently verified by unquantifiable means and can be classified within two categories of failure. This project investigates and analyzes possible sensor technologies that can provide in-process data to objectively quantify the characterization condition. Implementing in-process monitoring technologies will provide objective, quantitative evidence, prevent failed builds due to improper powder layer setups.the final solution for this project incorporates the use of both a 2D laser line sensor and an AM in-machine camera, this thesis will specifically focus on the in-machine camera. More specifically, this thesis will discuss camera repeatability tests that were conducted, the images taken during these tests, and the resulting pixel intensity values from these images. Analysis of the intensity values demonstrated that the in-machine camera could distinguish between different powder layer thickness values and that intensity values could be used as a quantitative metric to indicate whether certain powder layer characteristics are within specification.

This page is intentionally left blank.

Acknowledgments

I would like to thank our advisor, Professor David Hardt, who provided us with important technical advice that challenged us and led us to consider our project from diverse perspectives. I would also like to thank Jose Pacheco for all his administrative efforts this year. Additionally, I'd like to thank my peers, Jayna Wittenbrink, Satvik Sabarad, and Jane Modes for their support and hard work on our project. Moving to a new state for the summer and getting accustomed to our surroundings while tackling a fast-paced and technically challenging thesis project was not easy. Their determination and day-to-day words of encouragement were a huge source of motivation to me this summer.

I'd also like to thank the people closest to me for their relentless support, not just through this thesis project, but throughout my time as a student from high school to graduate school. I am grateful to have chosen MIT for graduate school, not just because of the incredible caliber of education, but because of the people I met there. In one year, I was able to meet and develop relationships with people who deeply understand and support me and I am really thankful for that. I would also like to thank my best friends who, despite being spread across the country, have been my daily support system since we were 16. Finally, I'd like to thank my parents and older sister who have always championed education and curiosity and hard work. Without them and the environment I grew up in, I am sure I would not be who I am today.

This page is intentionally left blank.

Chapter 1: Introduction

The broad objective of this thesis is to improve data acquisition during a machine setup for an additive manufacturing process. The specific aim of this project is to design a measurement system that can characterize an important powder layer property for additive manufacturing.

1.1. Additive Manufacturing

Additive manufacturing (AM) allows for the creation of complex geometries which cannot be created with traditional manufacturing methods. This is appealing to industries looking to improve service performance [1]. This process also allows parts to be manufactured with a high level of customization and reliability. Additive manufacturing, also known as 3D printing, creates parts by fusing or depositing layer by layer of material to form a complete part. Numerous technologies fall under the umbrella of additive manufacturing, and parts can be produced from various materials.

1.2. The Importance of Characterization in Additive Manufacturing

With any additive manufacturing process, achieving a successful characterization of certain powder layer properties is critical to the quality of the final part. Often, many parts are built at the same time within the build platform. If powder is deposited unevenly, this will produce inconsistencies in parts across the batch which could lead to performance issues. If the powder is too thick, for example, the laser beam may not fully penetrate through the layer of powder into the part beneath, resulting in a part that fails process verification tests such as tensile testing. If too thin, it is possible that the part being printed on could warp from the heat stress introduced by the print laser.

1.3. The Manufacturing Process

Powder characterization will be defined in generic units to protect the intellectual property (IP) of the project. This project aimed to investigate a powder layer of 1 to 3 units. This specification was treated as part of a defined parameter set meaning it could not be changed regardless of its importance to the performance of the final product.

1.3.1. The Current Quality Check

In typical additive manufacturing, important powder layer properties can be verified by unquantifiable means that fit within two categories of failure. The first is gross powder defects across the build plate. The second is uniformity in the powder layer.

There are a number of different gross powder failure conditions that can occur within powder layers. The current process check can identify several failures that can occur during printing and require adjustment of the setup. One common failure mode in additive manufacturing is caused by short feeding. Short feeding occurs when there is not enough powder being spread across the build plate. Other failures can include an inconsistent powder layer and powder clumping. These defects could be found during the process check or at an on machine monitoring camera to check for these defect conditions.

Once the issue of macro powder defects is taken care of, the second step in the process check, which is to verify whether important powder layer properties are within specification, is performed. A concern with this process check is that it is based on subjectivity. It is preferred to define quantitative measurement checks for such critical tolerances.

1.4. Problem Statement

As additive manufacturing processes begin to mature for use as industrial mass-production equipment, the tools to monitor parts during production need to develop as well. The use of existing approaches prompts the need for more specified monitoring equipment to ensure the production of safe, high-performing parts. This project aims to create a tool that could be used to objectively quantify a pivotal powder layer characteristic, powder layer thickness, in the AM process. This project investigates the possible sensor technologies and strategies that can provide in-process data to objectively quantify an important powder layer condition, along with the varying advantages and shortcomings of each. The manufacturing process requires a powder layer thickness on each part to be between 1 and 3 units.

Identifying and analyzing gross powder defects are not part of the project scope. We assumed that all powder anomalies which were discussed previously were not occurring or would be fixed before our tool performed an analysis of the characterization. If such powder anomalies were actually occurring, then our analysis would not be useful since the consideration of powder layer thickness would be a secondary concern to gross powder defects in the powder bed.

The ideal solution would take advantage of the existing hardware, software, and space available in an AM machine without interfering with the working space available. The most effective approach would be built out as an add-on module that can be used on any AM machine. Implementing in-process monitoring technologies for characterizing the powder layer will provide objective evidence and possibly improve machine throughput by reducing the time required to set up an AM machine for a build. While quantitatively measuring the characterization could assist during set-up, identifying and fixing the cause for a poor characterization set-up is not the main objective of

this project. The scope of this project is to deliver a proof-of-concept functional prototype which could be installed and tested on one 3D printer.

For this project, it is important to come up with a quick and cost-effective method of verifying a proper setup. The final tool should not cost more than the benefits of using the tool are worth. This solution should provide objective evidence to show that the specification meets design and process requirements.

1.5. Prior Work

Prior to the start of this project, other related projects were completed. The results of these prior projects influenced the project approach, but will not be described in detail.

The prior project involved a Keyence CL-3000 Series confocal laser displacement sensor. The sensor can be used to detect the distance from a zero setting to the object at which it is pointed. The sensor was used to measure the distance between the end of the recoater blade and the build platform. A few iterations of mounting equipment were developed to mount the laser system in the machine. The system was mounted on the recoater assembly of the 3D printer so that the point sensor could be used to take a line measurement across the entire build platform. With proper calibration, this data would produce a sample of expected powder layer thickness across the build platform, assuming that the powder height fell exactly at the bottom surface of the recoater blade. This system served as a starting point for the project.

1.6. Collaboration with MIT

This project was completed as part of the Master of Engineering in Advanced Manufacturing and Design at the Massachusetts Institute of Technology (MIT). All four team members worked

collaboratively, especially at the beginning stages of the process. After a broad evaluation of possible powder characterization techniques, which are outlined in Chapter 3, the team devised a solution strategy and split the work. More information on this is contained within the shared Introduction section of the Methodologies. This thesis will focus on the characterization of the onboard machine camera. Much of the content in Chapters 1 through 5 are common among the individual theses. The related work is documented in the MEng theses of Jayna Wittenbrink[1] with a focus on using displacement sensors to quantify the thickness of powder layers, Jane Modes[2] with a focus on detailing the results of various optical in-process monitoring tools, and Satvik Sabarad[3] with a focus on compiling the work from all theses to create a verification tool.

[1] J. Wittenbrink, "Using Displacement Sensors to Characterize Critical Powder Layers in Laser Powder Bed Fusion" thesis, 2022.

[2] J. Modes, "Optical In-Process Monitoring Tools for Laser Powder Bed Fusion: Verifying Powder Area Coverage of an Initial Layer Setup," thesis, 2022.

[3] S. Sabarad, "Comparing Various Methods for Validation of the characterization in an LPBF process using Optical and Displacement Sensors," thesis, 2022.

Chapter 2: Overview of Existing Monitoring Tools

While additive manufacturing is growing in popularity, few companies are scaling to large volume production using additive manufacturing. As such, there are not yet defined process and component certification methodologies for additive manufacturing [2]. The American Society for Testing and Materials (ASTM) and the International Organization for Standardization (ISO) have released some guidelines for additive manufacturing which are very broad and allow for much flexibility in the manufacturing process. With no defined standards, companies turn to trial and error manufacturing and testing using in situ process monitoring methodologies [2]. The following section describes the most commonly used methods in AM to monitor the quality of parts during production. Due to the specific focus of this project, many of these methods are not directly applicable. However, the condition of the powder bed is an important factor in producing mechanically robust parts and has been studied in more detail [3]. The different sensor technologies studied to this end are introduced in the second section of this chapter.

2.1. Traditional Quality Controls for AM

Current production tools are capable of monitoring many potential sources of variation in additive manufacturing. While some real-time, closed-loop control systems exist, most collect data during production that is analyzed afterward. For our purposes, achieving in-process control is not critical since a process check would be performed before printing begins. The most commonly used monitoring tools utilize optical and thermal techniques to track spatial variations and defects across the build surface over time [3; 4]. Optical imaging tools are advantageous since they provide a large amount of data, do not require contact with the parts, are non-hazardous, and have relatively large working distances [5]. Thermal sensors are usually used to measure features of the melt pool, while

optical sensors can capture a large variety of data [6; 4]. For example, 3D printing companies Velo3D, Aconity3D, and Concept Laser all have optical systems for powder bed monitoring, and thermal sensors to monitor the melt pool [6]. Similarly, the AM machine used for this project is equipped with cameras, reflectivity sensors, oxygen sensors, and pressure sensors. Acoustic monitoring tools are also increasing in use. For example, Renishaw's InfiniAM Sonic system determines the location of defects within the build using four ultrasonic sensors located under the build plate. Many companies also monitor the scanning laser itself such as SLM Solutions's Laser Power Monitoring system and Renishaw's LaserView module [3].

Several companies are working on software monitoring tools specifically geared towards additive manufacturing. Such simulation software packages are typically used to identify issues in an AM build due to the high strain and cooling rates that a part undergoes during the AM building process [5]. Other software tools, such as PrintRite3D from SigmaLabs use thermal imaging and machine learning to detect defects in real-time for AM [7]. SigmaLabs has been able to validate the results of PrintRite3D against results from X-Ray tomography [8]. The AM machine used for this project is equipped with DMP Monitoring and DMP Vision software which can be used to manually inspect images and thermal maps of each scanned layer [6]. All of these tools are designed to detect defects during the building process.

None of the above systems are able to directly measure a 1 to 3 units powder thickness. The optical solutions are generally built to detect defects on the millimeter scale and can only visualize surface features [5]. Optical imaging techniques could be used for powder layer setup monitoring, but the on-machine camera images from our AM machine are not sufficient in their raw form owing to poor lighting and inconsistent image quality from machine to machine.

A few companies have focused systems aimed at powder layer verification. SigmaLabs has performed multiple case studies to show that their PrintRite3D system can use thermal measurements to show the proper powder layer setup in a 3D printer after scanning with the laser [8; 9]. However, this validation will not be acceptable with the quality applicable for this project. Concept Laser's QM Coating system varies the amount of powder spread for each layer by using feedback from high-resolution cameras [10]. "An intelligent algorithm" makes a decision based on the subtraction of before and after powder images [10]. This tool is only available on Concept Laser systems so it cannot be used for this project. One of our approaches follows a similar method. Open Additive's Panda system also offers a high-resolution recoating imaging solution that they offer as an add-on for integration into other machines [10]. To find a new sensor to fulfill our requirements, we completed a thorough exploration of many different sensing methods. The overview of these explorations is discussed in the next section.

2.2. Non-Destructive Powder Bed Monitoring Tools for AM

Research on sensors that can more closely monitor powder bed conditions is available for a much broader range of sensor types than the more popular thermal and optical techniques described above. The initial review of sensor types is described here and is categorized into devices of optical, thermal, or acoustic nature. There are numerous types of sensors with unique operating principles, and this exploration is not exhaustive. However, we were able to disregard certain categories of tools given our particular project constraints. From there, we determined the most likely candidates for a deeper literature review, which is included in the Sensor Evaluation section.

2.2.1. Optical Imaging and Radiography

Optical sensors detect wavelengths of light between 100 nanometers of the UV range and 20,000 nanometers of the near-infrared (NIR) portion of the electromagnetic spectrum (EMS) [12]. Sensors operating in the X-ray portion of the EMS were also explored. Preliminary explorations removed UV, radiography (X-ray imaging), and time of flight sensors like Lidar from our considerations owing to insufficient accuracy [13; 9; 14].

In ultraviolet (UV) photography, only radiation from the ultraviolet (UV) spectrum is used to capture images and the wavelength of this spectrum ranges roughly from 10 nm to 400 nm. In reflected UV photography, the subject is directly lit by UV emitting lamps (radiation sources) or by bright sunshine. The lens has a UV transmitting filter on it that lets only ultraviolet light through while absorbing or blocking all visible light and infrared light [15]. This technology is mostly used in the medical field and the literature lacks evidence of this technology being used for a case similar to our purpose. Accordingly, this was not considered for further evaluation.

X-ray imaging is commonly used in additive manufacturing to check the quality, more specifically the internal porosity, of parts after they have been built and post-processed [16; 17]. X-rays have been used to take measurements with accuracy down to hundreds of microns, which is not sufficient for this project [18]. In addition to the lack of accuracy, exposure to X-rays introduces a health and safety concern for users of the equipment [18].

Lidar, or Light Detection and Ranging, emits pulsed light waves to the surrounding environment that bounce off surrounding objects and return to the sensors [19]. The distance to an object is calculated by the time it takes each pulse to return to the sensor [19]. Lidar is ideal for sensing non-stationary objects, such as a pedestrian on a sidewalk being sensed by an autonomous

vehicle [20]. Lidar has many uses but does not have the micron accuracy necessary for this project [20].

While NIR and Infrared optical cameras improved the accuracy of melt pool data, especially in combination with visible light cameras, we concluded that their accuracy on pre-scanned powder would be insufficient [8]. In NIR spectroscopy, light is cast onto the target substance with a broad spectrum of near-infrared light. This broad spectrum refers to light of many frequencies and wavelengths. The near-infrared light could be absorbed, reflected, or scattered by the target substance. Because of this, NIR posed an issue in our application [21].

The use of a digital camera, especially the one already in the machine, would be ideal for reasons described earlier, so we did a more thorough review of their use on powder monitoring in production. Digital cameras record the amount of reflected visible light received at the sensor. Variations in lighting and the reflectivity behavior of the material will vary the resulting intensity values received by a camera. On the other hand, laser triangulation responds to the physical geometry of the subject by detecting the angular displacement of reflected light [22]. Laser scanners use the same principle, but disperse the laser into a line that can produce a 3D dataset when moved across a sample [23]. Both of these were chosen for further study in this application.

Topography, or profilometry, are techniques that characterize the features of a surface including shape and roughness, and different methods of optical nature can be employed [24]. Laser confocal microscopy is a popular method for high-resolution surface topography measurements [25]. The Keyence sensor used for previous tests is a white light confocal displacement sensor which works by splitting white light into different colors and detecting the most prominent wavelengths through a spectrometer [25]. We decided to test this sensor since it was available on-site.

Other methods of optical topography include shape-from-focus and structured light [26]. Some of the more accurate sensors including microscopes that use shape-from-focus principles are machines too large to be used within the build chamber or have a field of view that is too small. On the other hand, structured light has been used directly within the machine production environment, and showed promise for our application. For example, Li et al. utilized a variety of structured light called enhanced phase measuring profilometry (EPMP) to offset the bad lighting and other challenges of the production environment and saw improved processing speed and accuracy [27].

We also considered the 3D optical technique, stereovision, which mimics the human eye by calculating depth from two images [28]. In their study of the formation and behavior of thin dust layers on bag filters, Saleem and Kramer built a custom in-process stereovision system [5]. This required the use of markers for calibration and alignment across the surface being studied, which determines the achievable accuracy of the setup. The depth accuracy obtained here was 100 microns [5]. It has also been mentioned that there is difficulty in designing and implementing markers within the machine production area [28].

Tomography is a technique that involves producing 3D output from layers of 2D data that are generally collected with optical or x-ray sensors. It is distinct from topography since it provides a full 3D depiction including internal features instead of only capturing surface details. Optical tomography generally requires at least a partially translucent subject, but for AM, it is achieved by capturing images at each layer of the build. X-ray tomography techniques are used for very high-resolution post-production quality analysis. However, its integration into the production process itself is not yet feasible [8]. The most promising technology for in situ measurement with these techniques is optical coherence tomography (OCT) which can reach sub-micron resolutions [29]. OCT operates through the principle of coherence scanning interferometry that operates similarly to

ultrasound [8]. Several studies use an OCT setup that places the tool in-line with the scanning laser. The melt pool can be monitored during printing, and the powder bed can also be analyzed before printing. However, in all of these studies, the researchers had full control over the system including the design of the scanning laser, optics, controllers, etc. [30; 31]. Since we are developing a process that will need to be scaled up to pre-existing machines, the intrusiveness of such a setup eliminated this technique from further consideration.

2.2.2. Thermal Monitoring

Numerous types of thermal sensors from applications such as surveillance, search and rescue, and defense could be used [33]. Thermal sensors are easy to use and are becoming lower cost as they grow in popularity [33]. For this project, thermal sensors that require contact with the part such as thermocouples, thermistors, resistance temperature detectors, and temperature integrated circuits, were not considered [34]. However, non-contact thermal sensors, such as infrared thermometers, were considered for this project as we did not expect that the thermal map would change in a detectable way with the sub-millimeter scale of powder that would be deposited on the parts [35].

One thermal monitoring tool which was explored in more detail is flash thermography. Flash thermography is an active thermography method that uses a heat source to induce heat into a part and a thermal camera to inspect the part [36]. This allows for a high contrast thermal image to be created for a part at ambient temperature [36]. For our application, flash thermography was considered a tool to check the uniformity of deposited powder. It could also be used to correlate a thickness measurement in combination with another tool. However, after speaking with representatives from moviTHERM, it was determined that flash thermography was not the best option due to its low resolution, which would not be usable to detect the size of powder in our project, and its high cost. For this project, other tools like 3D scanners are better suited for the

application and are available at a fraction of the cost of a flash thermography system [36]. It is also unclear if flash thermography would lend the resolution and accuracy needed for the measurements we are aiming to take [36].

Other thermal monitoring tools may involve thermography and thermal cameras. Thermography can detect the variance in thermal behavior between a defect and the part [9]. High-speed infrared imaging can be used along with optical imaging to track deposition and predict the surface temperature during powder deposition, temperature gradients, and liquid-solid interface velocity. These can be used to understand the quality and microstructure of additively manufactured parts [7]. Conventional charge-coupled devices and near-infrared cameras have been used to detect porosity in additively manufactured parts [7]. These techniques have been shown to correlate with the results seen from 3D X-Ray tomography [7]. Like optical methods, post-processing of data is required for correlating measurement values to part features, though the emissivity of the powder bed will be highly variable depending on surface morphology, oxygen content, and how often the powder has been recycled, etc. [8; 9].

2.2.3. Acoustic

One newer method for defect detection in additive manufacturing is acoustic monitoring. The two main acoustic monitoring techniques for AM are ultrasonic testing and acoustic emission spectroscopy. Acoustic emission spectroscopy detects the acoustic emissions from the process laser, so it is not relevant for our purposes. Ultrasonic testing measures induced waves that are conducted and reflected through a part as it's being built [8]. An ultrasonic probe mounted underneath the build plate measures reflected acoustic signals that occur with sudden changes in density in the material [37]. This technique can be used to detect defects such as cracks and porosity [9]. We concluded that this would not be the right approach to measure loose powder to our desired accuracy.

2.3. Summary of Selected Technologies

After looking into a broad range of possible sensors, we determined the most likely to work within our project constraints. Table 1 displays an overview of all technologies considered, which were selected for further evaluation, and the reasoning behind that consideration. We decided to do a deeper literature review on additive manufacturing for digital cameras, laser triangulation sensors, confocal chromatic sensors, and structured light sensors.

Table 1. Below is a summary of various measurement principles and sensor types that were evaluated for our application.

Categories of Measurement Principles	Considered for further evaluation?	Reason
Optical + Radiography Methods		
X-ray	No	EHS concern, not accurate enough
Pulse Based (Time of flight)	No	Not accurate enough, not many articles are available on this technology
NIR	No	Not enough accuracy
Visible Light (Digital Cameras)	**Yes**	Provides a lot of information, large working distances, already integrated in the machine
Laser Triangulation	**Yes**	High accuracy and ease of use
Confocal Microscopy	No	Can't find a modular or portable one
UV Photography	No	Lacking evidence of use in a similar field; Primarily used in the medical field
Chromatic Confocal Sensor	**Yes**	Already available for testing on-site, high accuracy and precision
Structured Light	**Yes**	Has desired accuracy
Stereoscopic Vision	No	Requires use of precise markers in the measurement area for high accuracy readings
Optical Coherence Tomography	No	In-line assembly with scanning laser difficult as an add-on module
Thermal Methods		
Flash Thermography	No	Expensive, not enough accuracy
IR Imaging	No	Not enough accuracy
Acoustic Methods		
Ultrasonic	No	Not enough accuracy
Acoustic Emission Spectroscopy	No	Requires use of the acoustic emissions from the scanning laser

Chapter 3: Background Principles

3.1. Powder Spreadability

Powder spreadability over the build surface and the corresponding powder density greatly affect the mechanical properties of the final product [38; 39]. In characterizing the important powder layer properties, it is helpful to study the parameters that influence how the powder spreads across the parts. Features of the powder, the surface across which powder is being spread, and the recoating system, all affect the resulting powder coverage. Even though the specifics of the design such as recoater speed and part surface roughness cannot be altered, within the testing environment it is necessary to ensure that conditions are as close to a reasonable set of production conditions as possible.

Particle size distribution (PSD) and shape are some of the important powder qualities that affect powder density [38; 39]. To improve spreadability, the particle distribution should be narrow to reduce the interparticle friction that prevents flow [40]. The powder particles used in this project are particles of an alloy classified by their particle size (D10, D50, D90) [41]. For a homogenous powder layer coating, increasing the sphericity of the powder particles increases powder coverage [42]. While powder flowability is often equated to spreadability, Phua et al and Mitterlehner demonstrate that powders with worse flowability can have superior spreadability when a realistic surface is considered instead of the perfectly flat surfaces used in simulations [42; 44]. Their research shows that powder coverage increases nearly linearly with an increase in surface roughness between an arithmetic roughness of 8.5 and 25.3 microns [41; 43].

In addition to powder characteristics, features of the recoater system including recoater speed and the recoater gap will affect the powder layer. Generally, increasing the speed of the recoater results in less powder coverage and reduces uniformity [42; 44]. This project uses the manufacturer's standard parameter recommendation for recoating speed. The recoater gap is the distance from the bottom of the recoater blade to the surface over which powder is being spread. Ideally, when the recoater blade moves over the build plate, it spreads powder uniformly over the surface to the thickness of that gap. However, in reality, this does not happen because of a phenomenon called jamming.

Jamming describes a state of disordered particle systems when they behave as a solid, meaning that the system is mechanically stable when exposed to perturbation, rather than flowing like a fluid [43]. In the powder recoating processes, transient jamming occurs when the recoater gap gets too small, relative to the D90, or 90th percentile particle diameter. Regions of particles begin to stick together and reduce powder spreadability, essentially creating large bald spots by dragging the jammed clumps and larger particles across the build area [38]. Nan et al. [38] found that around a gap height of 1.5 times the D90 significantly increased the probability of these large empty spaces. This can cause serious complications to the final quality of the product because the patchy area coverage leads to weak bonding during the sintering process [29]. Jamming is important for us to consider because it has an effect on powder coverage and layer thickness because it can cause uneven spreading of the powder. Powder spreadability greatly influences pixel intensity values; it can cause an increase in intensity if there is an accumulation of powder or a decrease in intensity due to the previously mentioned bald spots. This was an important phenomenon for us to understand especially because certain powder defects and anomalies in intensity values could be attributed to it.

Chapter 4: Sensor Evaluation

4.1. Digital Cameras

Optical-based technologies are widely used to monitor the AM process. They are heavily used to identify defects and help in taking corrective action to avoid the part getting rejected in later stages. Digital cameras have been used to identify gross powder defects as well as sub-millimeter scale features across the build plate.

The more common application of external cameras is to monitor larger defects within the powder bed. Recoating defects perpendicular to the recoater blade movement were identified by Craeghs et al. by using an external camera system [44]. Scime et al. automated the detection and classification of anomalies in the powder bed using the EOS M290's stock illumination by using a 1.3 megapixel (MP) powder bed monitoring camera [45]. F. Caltanissetta et al. integrated a 10.5 MP camera into the build chamber laterally and combined it with ideal lighting conditions to get clear images of the build process. They also observed that diffused lighting helped them capture good images as compared to the direct reflection of light into the camera [46]. Furumoto et al. placed a Photron FASTCAM SA5 model 1300K C2 high-speed camera onto a custom AM machine to test a simpler, off-line method. They monitored the consolidation of powder during irradiation by placing a camera vertically above the powder bed to study the effect of altering powder layer thickness [47].

There is also research that studies the powder bed with higher resolution to identify smaller defects during the build process. Abdelrahman et al., identified different types of defects during the build process by focusing a 36 MP camera on a 250 x 250 mm build area (resolution of 45-88 microns per mm) [48]. They used optical imaging to study anomalies in the powder layer before laser scanning and in the solidified material after scanning. Correlating numerous pictures under

various lighting conditions and from multiple layers allowed the identification of lack-of-fusion flaws using optical data [48]. There was only one study where authors were able to achieve even higher resolution. F. G. Fischer et al. could identify features as small as 12 to 14 microns over a 98 mm width by deploying their own optical process monitoring system which can be mounted on the recoater blade [49]. Since this study showed promising results, we are considering more optical sensors with higher resolution for the study. These sensors will be mounted closer as compared to the existing in-machine onboard camera to reduce the field of view and thereby increase the resolution. This is the focus of Jane Modes's thesis, where she will specifically consider the results from a USB microscope, Spectral Instruments vacuum compatible camera, and other digital cameras.

We deeply explored the approach of using optical imaging for this project's application because we wanted to clearly distinguish between the powder and the part from the part. A common method for evaluating powder layers with a camera is to evaluate the percentage area coverage over the build area by distinguishing between the powder and surface below [42; 44]. For example, Wei Lin et al.'s work analyzed the quality of powder layers through image processing by just this method [50]. They captured many images from an optical camera and they further processed the images in MATLAB to convert those images into binary images (only white and black pixels). Two tests were performed on the samples that were acquired during the studies. The deposited powder layer's surface pictures were first digitized and visually analyzed. The percentage of black or white pixels in the picture was examined next to see if the layer had been distributed evenly. They also adjusted the threshold value before converting the images to binary to ensure the powder over the surface could be distinguished easily. Furthermore, they studied how powder spreadability is affected by the layer height and used binary images to evaluate the percentage area covered by the powder over the part

[51]. For example, in Figure 3, a 24 by 16-pixel image is displayed along with the intensity values. We can see that the value of a pixel is 0 when the pixel is completely black and 255 when the pixel is completely white.

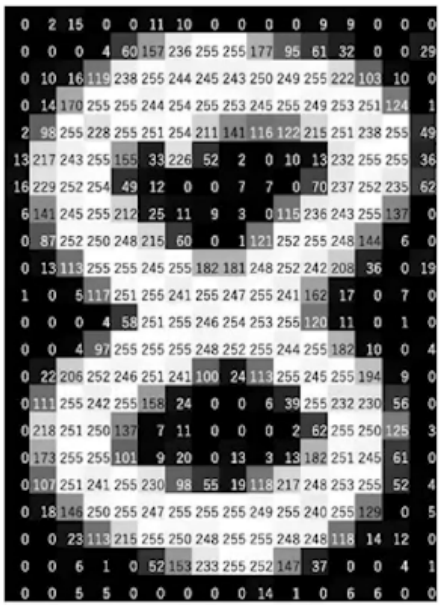

Figure 1. A 24 x 16 image with intensity values (ranging from 0 to 255) displayed on each pixel is shown above [52].

Pixel intensity values can be used to distinguish powder from the parts. As will be discussed in further detail in the lighting section within the Methodology chapter, the position of the lighting inside the machine is such that the light source is not in the “Family of Angles” [53]. This ensures that the part is not reflecting the light back into the camera. If we take a picture at this point, we will observe that the image is dark and the pixel values are in the lower range. However, when a layer of powder is spread on the part, the pixel values change because the powder is light in color and reflects more light into the camera. Since the powder particles are light in color, the intensity values increase and this helps us in distinguishing the powder from the part. This method has been discussed by Wei Lin et al., where they have demonstrated that the powder can be distinguished from the part using an optical technique [53]. As discussed earlier, a camera is already pre-installed

in our machine for in-situ monitoring but it is not being used for the quantification of the characterization. We will discuss in detail on how we used the images captured by this camera to quantify the characterization in the later sections.

4.2. Laser triangulation

Laser triangulation sensors are compact, non-contact 2D sensors that perform distance measurements by angle calculation. They are commonly used to measure thickness, even on the micrometer scale, with high accuracy [54].

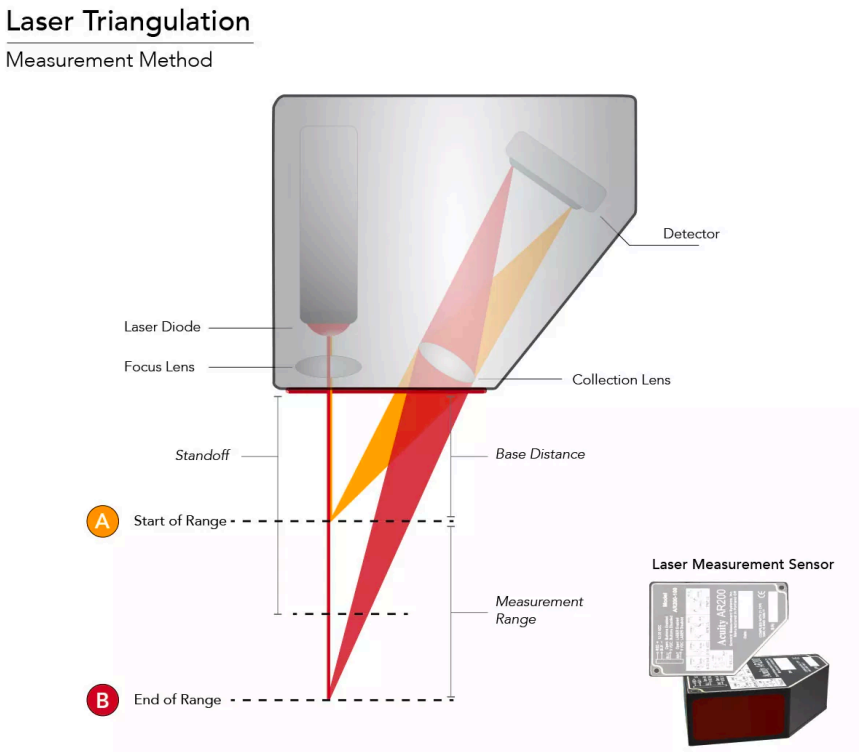

Figure 2. The principle of measurement in laser triangulation is demonstrated above [54]. In laser triangulation, a laser beam is projected from the sensor to the target and reflected in the collection lens. The laser emitter and collection lens are beside one another in the sensor enclosure.

There are two configurations of laser triangulation sensors: the point sensor and the line sensor. In a laser triangulation point sensor, the collection lens focuses on an image of the laser spot

on a linear array detector. The detector views the measurement range shown in the image above from an angle usually between 45 and 65 degrees, though this varies by sensor model. The location of the laser spot image on the detector's pixels is processed through digital or analog signals to measure the distance to the target [54].

In a laser triangulation line sensor, the laser projects a continuous line of light across the target. While the projected line does appear distorted, a detailed analysis of the distorted image allows for a highly accurate reconstruction of the object's shape. From this type of sensor, a 2D profile can be created [55]. Laser triangulation sensors can measure many different measurement ranges depending on the instrument model. These sensors can be used for any scale of measurement, but accuracy decreases as the measurement range increases. Both exposure and power levels of the laser can be controlled to improve accuracy based on outside factors like lighting [54].

To assess the applicability of laser triangulation sensors in the thesis project, various pieces of literature were reviewed. Donadello demonstrated the use of a laser triangulation sensor for process control of laser metal deposition [56]. Although this paper described laser triangulation for height monitoring for a different type of additive manufacturing known as laser metal deposition (LMD), it still provided important insights about using laser triangulation sensors in the printing process. The system described in the article uses optical triangulation, in a coaxial and non-intrusive configuration, for height monitoring on an LMD setup. A laser beam from the sensor enclosure is projected onto the melt pool and a coaxial camera, which is located adjacent to the laser beam in the sensor enclosure, obtains the laser spot and converts its position to relative height. In this paper, the laser triangulation device is being used for process monitoring of the deposition of a stainless steel cylinder. The ultimate output of the sensor is a spatial map displaying height variation in the melt pool [56].

Some of the main issues posed by the triangulation system used in the paper are that: (1) the system is used to monitor the height of a melt pool rather than loose powder and (2) that laser spot detection quality could deteriorate because of the target's reflectivity.Additionally, while the powder's appearance will be matte in the thesis project, the transparent layer will allow the reflective part to be easily visible. As mentioned in the paper, "spot detection might partially suffer from … target reflectivity," and this is another major issue that could come about from using laser triangulation for the thesis's objective [56]. This article provided valuable insights and context into how laser triangulation can be used in process control of additive manufacturing as well as some issues that could arise through its usage.

Another reading that provided useful information on the use of laser triangulation for in-process monitoring for additive manufacturing was "Novel machine and measurement concept for micro machining by selective laser sintering," [57]. In this paper, a Keyence 2D laser displacement sensor operating according to the principle of optical triangulation was used to verify the thickness of deposited powder layers as well as the resulting sintered parts. The spot diameter from the laser was 40 µm x 25 mm with repeatability on the x-axis of 5 µm and the z-axis of 1 µm, which matches the repeatability values necessary for the thesis project. The sensor is moved over the surfaces and after combining all the measured profiles, a 3D dataset is created. According to the source, this novel, in-situ method for process control, with further development, could be used in future direct in-process control [57]. A 3D measuring system was integrated to analyze the acquired data using a 3D topographic map constructed in MATLAB. For this paper, the main objective was to find inhomogeneities and surface defects in the deposited powder layer. The tools and approach produced useful results for the researchers and provided further parallels to demonstrate that a laser triangulation sensor could be viable within the parameters of the thesis project. Laser triangulation

sensors are not often used on reflective surfaces because the laser light “would bounce directly back onto itself” [58]. The accuracy of a laser from a laser triangulation sensor on a reflective surface is challenged because the surfaces produce a distortion of the reflected beam called the speckle effect. The speckle effect is caused when the laser light is intermittently coherent and is scattered from a random, non-homogenous surface. This surface would cause small waves to overlap in the air after leaving the surface, leading to the speckle effect [59].

Along with the reviewed literature on laser triangulation, it was found through general research that one of the most popular applications for laser triangulation sensors is the measurement of thickness. Particularly in contexts like inventory management or quality or process control, which relates to this project, laser triangulation sensors can provide precise thickness measurements and have begun replacing tools like manual contact gauges and Linear Variable Differential Transformer (LVDT) sensors [59]. Another relevant aspect of these types of sensors is their ability to measure in the correct scale of units. Since the powder layer is to be within 1 to 3 units, the sensor used here must be able to detect in the micrometer range, and some laser triangulation sensors can do so, which provided further evidence of their viability.

Acknowledging that the reflective surface of the part and the speckle effect could pose some issues for the thesis project, the group decided to move forward and try out a laser triangulation sensor on the experimental setup in our project’s machine. The MicroEpsilon scanCONTROL Sensor is a laser triangulation line scanner that, as described above, can construct a 2D profile of the target by projecting a line of light on the target. The optical system within the sensor projects the reflected light of this line, which is diffused, onto a sensitive sensor matrix. Using the matrix image, the sensor’s controller calculates the distance, along the z-axis, and the position along the laser line, along the x-axis. There is then a 2D coordinate system produced to construct the resulting 2D profile

[59]. This system was then mounted on the recoater unit to produce a 3D representation of the surface.

4.3. Structured Light

Another type of sensor considered during preliminary research was the structured light sensor. Structured light imaging has the "potential for micrometer-level 3D measurement" and is commonly used in machine vision applications due to its high-resolution capabilities [60]. Structured light imaging sensors are able to capture 3D topographies of surfaces using a particular pattern of light and a 2D imaging camera. The pattern is projected onto a target object and as the camera observes the pattern from various perspectives, the target object's surface features distort the projected pattern. This distortion is then used to reconstruct the 3D topography of the target object [61].

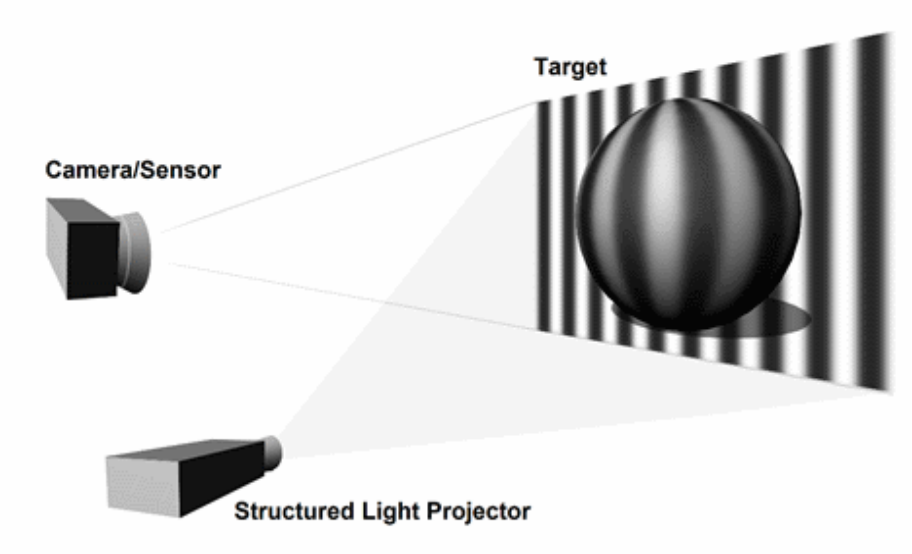

Figure 3. The principle of projecting a pattern on a target in structured light imaging is shown above [60].

The example above demonstrates a sine wave intensity pattern being projected onto a spherical target object [61]. In the context of the thesis project, with a 3D topography, the relative height of the powder layer on the part could be obtained using this projection method.

One piece of literature that provided insight into the use of structured light imaging in additive manufacturing is Zhang et al. 's “In situ Surface Topography of Laser Powder Bed Fusion Using Fringe Projection” [61]. This paper presents how structured light imaging fringe projection is used to detect the surface topography of powder bed layers. The two major parts of the fringe projection system in the paper are a camera and a projector. The projector creates the structured light patterns on the target object’s surface, which is the powder layer, and the camera takes images of the patterns from various perspectives. As previously explained, the projected fringes will become deformed by the variations of the surface’s features, and these deformed fringes are then used to get the surface topography [61]. The main components of a fringe projection system are a projector and a camera. The projector can produce structured light patterns (e.g. a sequence of sinusoidally varying intensity patterns) on the surface of the object, while the camera captures these patterns from a different viewing angle. The projected fringes appear deformed due to local height variations of the object surface. The deformed fringes captured by the camera are then reconstructed to obtain the 3D shape of the object [61].

In Zhang’s setup the laser and scanner were placed directly above the processing chamber to take measurements and capture images as the print progressed. For our project, if a 3D scanner were to be used, it would likely be mounted on the recoater unit, in the same chamber as the printing part. Mounting the scanner above the build chamber would likely require further configuration. This is because the port in which the scanner would sit is at an angle, rather than straight above the build plate.

One issue with structured light imaging that is also found with laser triangulation is that of the speckle effect, as previously discussed. This effect is sometimes seen with certain surfaces for fringe projection, which would cause the 3D topography not to be accurate due to oversaturation of some pixels. The researchers in this paper were able to identify the saturated pixels and remove them from the data set before reconstructing the topography [65]. By performing structured light imaging on powder layers and adequately overcoming issues caused by reflective surfaces and the speckle effect, this paper presented a promising application for structured light imaging in the thesis project [61].

Another paper to support the use of structured light imaging in the thesis project is “In Situ 3D Monitoring of Geometric Signatures in the Powder-Bed-Fusion Additive Manufacturing Process via Vision Sensing Methods” [27]. In this paper, the 3D surface topography of a powder bed was monitored using structured light imaging. Specifically, multiple sinusoidal fringe images were projected on the powder bed and two cameras captured the images at the same time. Using the topography, researchers were able to monitor for homogeneity and defects. The same image-capturing process was applied after laser exposure to find the topography of the fusion area.

The main issue the researchers encountered is that the entire process of detecting and classifying defects is very manual. The system in place can take important measurements, such as the height profile, through manual selection, but would require machine learning techniques to be able to make the same detections in an automated way. While this study does not specifically state the kind of powder used, there is no mention of reflectivity issues , and the powder is not being printed atop a reflective part, as with this project [27]. Overall, this paper provided insight into another case in which structured light imaging could be used for height measurements of a powder layer in AM.

Other than the issue of the speckle effect, the literature reviewed provided strong evidence for the applicability of structured light sensors in the MIT thesis project. In particular, these sensors are able to capture a 3D topography of the target surface which provides a more complete view and therefore more comprehensive analysis of the surface under consideration. Additionally, the literature showed that structured light sensors were successful in an AM process, providing further credibility for its use. Because of this, the group decided to move forward with trying out a few different structured light sensors. The different scanners that we acquired for demonstration purposes will be explained in Jane Mode's thesis.

4.4. Confocal Chromatic Sensors

The confocal principle uses a single-point light source to measure only the reflected light from a surface that is in focus [62]. Confocal microscopy is a popular method for determining surface roughness including for AM produced parts, but the machines are large and bulky as they are meant to be used in a post-production quality analysis environment [63]. Confocal chromatic sensors, also referred to as white light or multi-color confocal sensors, use a variation of the confocal principle that splits the point source light into different wavelengths, or different colors through a series of lenses. The reflected light can then be analyzed for the wavelength that is most in focus through the use of a spectrometer. This eliminates the need for electronics within the sensor head which greatly reduces the size of the sensor and makes it usable in vacuum environments [64]. Sensor manufacturers laud the increased stability, precision, and accuracy of their confocal chromatic sensors even on difficult surfaces including transparent, high roughness, and tilted surfaces [65].

The use of confocal chromatic sensors within AM is not as common as other optical techniques. Their advantage in measuring through transparent media makes them more popular in the biological sciences. Scanning systems allow the point sensor to recreate 3D models of samples which can take about two hours to build for a window of 2.1 mm by 0.95 mm [66]. Yang developed an in-process confocal scanning imaging system with a fiber transceiver for laser powder bed fusion to characterize the powder and solid material within the print bed [67]. They reported successful imaging even with the high scattering of the loose powder surface, though they mentioned the need for further work on verifying these results in terms of surface roughnesses. Despite the lack of directly applicable research in chromatic confocal sensors for AM especially for the characterization of loose powders, we decided to test the Keyence CL-P030 due to its previous use for the same powder layer characterization process.

Chapter 5: Methodology

5.1. Introduction

The advantages of using digital cameras are highly appealing because of their ease of use and the wide availability of image processing software. Since the digital camera on the machine, referred to as the onboard camera, had not been analyzed thoroughly to determine its viability for our project's objective, we decided to focus the crux of our research, and eventually our solution, on this camera. Since the original specification calls for an unquantifiable process check, onboard camera results were compared to this input to determine if pass/no-pass thresholds could be determined from the camera. I took the lead on this part of the project. However, within our purpose of more objectively quantifying the powder layer, we also deemed it valuable to use sensors that could provide more accurate results to characterize the layer. Jane Modes and Jayna Wittenbrink tested and analyzed the results from the sensors chosen in Chapter 5: optical devices in Jane's case [68] and laser displacement sensors in Jayna's [69]. The goal was to correlate the values between all these results to provide an actionable result using solely the images of the onboard camera. This meant that the auxiliary sensors tested by Jayna would be for testing purposes only, and not meant for regular use within the process. The correlation between the MicroEpsilon sensor and intensity values as well as the comparison between the set intensity limits and a machine learning algorithm, both based on the current process check, are detailed in Satvik's thesis [70].

5.2. Overview of onboard camera analysis

The focus of this thesis was to test the onboard camera and determine the best way to process the images to characterize the powder layer. The camera was used to take images and videos of the

build plate. From these images, intensity values were computed for every part using an image processing software called ImageJ, and were found to vary based on powder thickness. An intensity value is defined as the mean gray value of an image, which is the sum of the gray values of all the pixels in a selected area divided by the number of pixels [71].

We found that with sufficient replicates, the difference between mean intensity values for successive powder layers, increasing in increments of 0.25 units, was significant at a 90% confidence level. This signified that the onboard camera was able to identify the difference between powder layers via intensity values. This led us to choose intensity values as one method for characterizing the powder layer.

We also found that mean intensity values increased as the powder thickness on the build platform increased. During these tests, we also gained feedback through the current process check on whether each part at every tested powder thickness would be considered a pass or a no-pass. We considered the current process check outputs as our "source of truth." We then found the intensity values of all the parts in this test and matched them to the current process check output data. From this, we established pass/no-pass intensity thresholds. A more in-depth description of these results is found in the Results and Discussion section.

5.3. Onboard camera

The onboard camera is located in a glass-shielded port above the build chamber in a secure enclosure. It is able to provide an area scan of the entire build plate, but since the port is positioned at approximately a 45 degree angle 9 inches above and 4 inches to the right of the build plate, the images it takes of the plate are at an angle.

The camera uses CMOS sensor technology and provides live footage in the build chamber. This makes it an economical solution that would not require a plan for configuration and a necessity for validation, unlike if a new camera were implemented. Prior to using the onboard camera for testing and analysis, however, there were some significant issues to be addressed.

For example, when settings such as the exposure and light diaphragm were adjusted, this was reflected in the machine's monitoring software. However, once the images were saved locally, these adjusted settings were no longer reflected. Additionally, we encountered issues with uneven lighting across the build plate, which made it difficult to distinguish between the parts and the surrounding build plate. All these issues posed a significant hindrance to producing accurate results from image processing.

5.4. Method for producing analyzable images from the onboard camera

To fix camera alignment and lighting issues and produce images that would give us accurate results, we performed different types of calibration, adjusted exposure and light diaphragm settings, and conducted lighting tests. Once we were able to find a permanent fix that could be replicated in additional machines, we confirmed our choice of this onboard camera.

5.4.1 Camera Calibration

Camera calibration is performed to determine the specific characteristics or parameters of a camera to accurately relate the 3D points being captured and the 2D project in the image taken by the calibrated camera [72]. For our project, calibration was done to the onboard camera prior to beginning testing and when misalignment was detected. According to the machine's user manual,

the steps for calibration include checking the camera installation, calibrating the light budget, configuring the camera exposure, calibrating the lens focus, and performing the perspective calibration.

5.4.2 Lighting

When first testing out images with the onboard camera, we encountered many issues caused by uneven lighting. The original position of the light induced a lot of reflection, leading to images with excessive glare. When attempting to process these images, ImageJ erroneously identified the glare, which appeared nearly white, as powder, even when the build plate was completely clear of powder.

We realized that we either needed to adjust the position of this light, replace this light or increase the overall amount of light in the machine to fix this reflectivity issue.

In our application, we wanted to distinguish between powder and the part beneath the powder. If the source of light lies in the "Family of Angles" as shown in Figure 8 a surface will appear to have increased glare in resulting images. We wanted to avoid this type of glare because it would make it difficult for ImageJ to distinguish between the powder and part. Hence, we decided to place the light source anywhere except in the zone of the "Family of Angles."

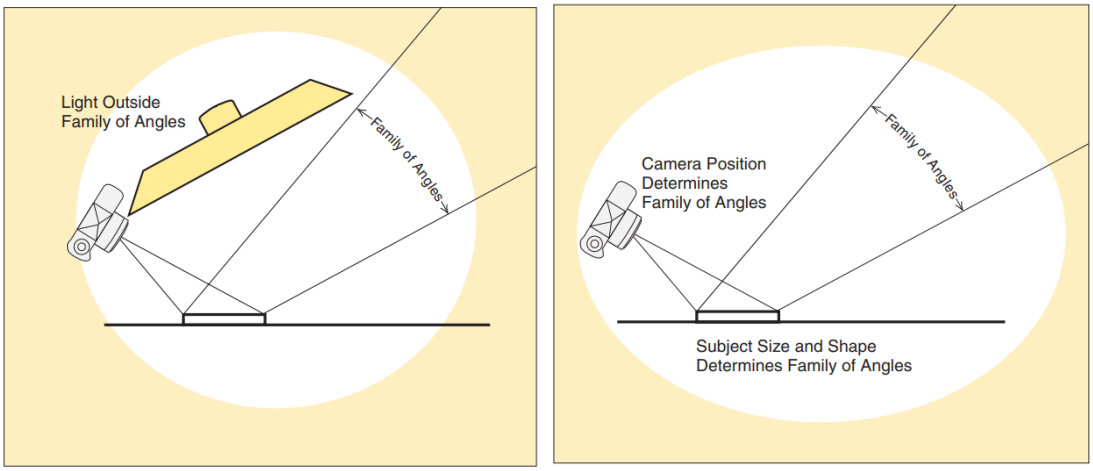

Figure 4. Keeping the light source in the "Family of Angles" directly illuminates the target object and the light is reflected into the camera but keeping light outside the Family of Angles to keep the target object dark [57].

Using insights from this research, we began performing lighting tests. Our first step was finding the optimal position of the existing lighting bar. Our research indicated that placing the light in the Family of Angles, as shown below, would cause a lot of reflection and glare. To corroborate this, we placed the lighting bar on the opposite end of the machine from the camera, in the horizontal direction, and took test images. As predicted, this lighting position worsened the glare.

We then placed the pre-existing light on the same side of the machine as the camera, only 4 inches below the camera. With the light positioned far out of the Family of Angles, the images now had far less glare. This lessened glare was not as pronounced with a build plate completely clear of powder, as is shown below, compared to a build plate with clear parts and packed surroundings. However, once the clear parts were surrounded by powder, referred to as a packed build plate, the reflection on the side of the parts was also eliminated.

The use of a diffusion material when it is difficult to place the source of light outside the Family of Angles was also discussed in the research we conducted. One way to avoid direct illumination, which can more easily cause reflectivity, is by adding a diffusion material in front of the light source. Diffusion materials can include acrylic sheets, polycarbonate sheets, or even just a piece of paper. The purpose of the diffusion material is to soften the strength of the illuminated light.

Although we were able to place the lighting bar outside the Family of Angles, we also wanted to try to pursue the use of diffusion a bit further to see its effect. While covering the onboard camera with a white piece of paper did greatly decrease the glare in produced images, the result dimmed the images so much that it was again difficult for ImageJ to distinguish between the powder and the parts.

After concluding that the non-diffused preexisting light, positioned on the same side of the machine as the camera, produced the most optimal results, we wanted to test whether adding other lights to this setup would help. We tested three additional lighting options including an LED Colored Ring Light, a light panel with different color diffusion sheets, and an LED-colored rope light. For each of these lights, we used the red-light option, since red has the lowest refractive index, and placed each light on the same side of the machine as the camera and the original light bar. While none of the lights increased the reflection and glare on the build plate, they also did not help the result drastically. Because of this, we decided to just use the preexisting light, since this would be most economical and convenient, especially if the solution scales.

Once we settled on which light to use and its position, we acquired an additively manufactured mount for the lighting bar that is adjustable in its vertical position and angle relative to the build plate. We attached the light mount to the right-hand side of the machine on a preexisting vertical bar.

We then began taking test images and determining which other settings could be adjusted so we could produce the best images possible. We found that the exposure setting and the light diaphragm affected the brightness and contrast of the produced images. We ended up setting the light diaphragm to allow as much light as possible to enter. This provided a lot of brightness and contrast to the image, making in-process monitoring and distinguishing the powder from the part in image processing more efficient.

5.4.3. Taking Videos and Converting to Images

We took 10-second videos of each layer to combat the issue previously mentioned with the misalignment portrayed in the images taken on the machine's live view of the build plate. We found

that taking a video and extracting an image from each video using VLC Media Player gave us high-resolution, properly aligned images suitable for processing and analysis.

5.5. Camera Repeatability Tests

Once we determined the optimal conditions and procedures for taking images using the onboard camera, we began our experimental process for characterizing the characterization using intensity values. Referred to as the Camera Repeatability Test, we planned to take images of different powder thicknesses on the build plate and analyze the intensity of each part in each powder thickness. We wanted to concentrate on important "boundary" thicknesses, which were the lowest and highest values within the specification range and 0.25 units above and below those low and high values. From finding the intensity values at these boundary thicknesses, we would be able to tell whether the onboard camera could distinguish between powder layer thicknesses that only differed by 0.25 units.

Our procedure consisted of taking images and videos, using the machine monitoring software, of the packed build plate from 0 to 5 unit powder layer thickness, increasing the thickness in increments of 0.25 units. For each layer, we used the current process check to check which part was "good" or "bad". Good or bad referred to whether the part would pass the qualitative check done with the current process check.

Going from 0 to 5 units in layer thickness was called one full setup. We did 10 setups to get a substantial amount of replicates. After each setup, we cleared the build platform of powder before starting on the next. This 0 to 5 units range covered both the specification range for the powder thickness and increased in small enough increments to be able to track changes between layers both

qualitatively and quantitatively. We kept the machine light on and closed the machine door for all setups. We did not change lighting conditions throughout the entire test.

While performing these tests, we encountered several issues. First, the recoater blade was getting easily worn out which caused issues with uniform powder spreading. Second, since each part has its own tolerance, it cannot be guaranteed that parts sit exactly flat or at the same height on the build platform. As a result even if the build plate powder thickness was within specification, some of the parts would not pass the qualitative process checks.

We decided that we needed to redo these tests, but first make some necessary changes to our equipment and process. We modified our procedure to have the recoater blade replaced after every setup to avoid excessive wear. However, once we replaced it, we noted that we also needed to redo the entire process required to set up the characterization. We also had our first build plate replaced to fix process issues. With all these changes made, we began our second round of testing.

Once we finished with these tests, we moved to analysis. We had three main objectives for our analysis. First, we wanted to see if the onboard camera could identify the difference between successive layers, particularly at the important boundary layers for the thickness specifications. Second, we wanted to use the current process check to determine which part was passable or not for the layer thicknesses within specification. Third, based on the current process check output, we wanted to determine a range of intensity values at each part position that can be used in the final verification tool.

5.6. ImageJ Analysis

Our main tool for image processing was ImageJ [75]. Developed by the National Institutes of Health and a common image processing tool for biology applications, ImageJ was useful in our

project since it had the ability to detect very fine particles, like the powder we worked with, in images.

We began our analysis by determining how we could distinguish the powder from each part to analyze it. We were interested in studying area percentage coverage and intensity, as these were two values often analyzed in literature about powder coverage. We were able to isolate the powder from the part through image subtraction. For subtraction, it was necessary to take a picture of the build plate with parts completely clear of powder as well as a picture of the build plate, in the same exact position and lighting, but with whichever layer of powder was to be studied. By subtracting the image with powder from the completely clear image, the background would no longer exist and only the powder would be visible.

Thresholding is the conversion of an image to grayscale followed by segmenting the image into a binary set of pixels. We needed to do thresholding prior to calculating percentage area coverage so that the processor could establish which pixels should be white, to demonstrate the powder, and which pixels should be black, to demonstrate the part.

We tested different versions of thresholding, including simply using the auto-threshold function on ImageJ, greatly increasing the contrast on the image and then placing auto-thresholding, manually adjusting the threshold to match the image, and applying a histogram equalizer before selecting the auto-threshold. In the auto-threshold, the “IsoData” algorithm is used, in which the image is divided into an object and a background by taking an initial threshold. This is followed by the averages of the pixels at or below the threshold and pixels above being calculated [75]. However, we soon realized that the threshold must be different for every part on the build plate. Applying any kind of default threshold was not allowing ImageJ to properly delineate the powder from the part for every part on the build plate since powder coverage varied by location. We resorted to manual

selection and manual adjustment of the threshold for each part. We could not find any consistent trend in the percentage area coverage. This could be because of the lack of resolution of the onboard camera or the images used or because there actually is not a consistent trend. We did not pursue this further and instead moved to intensity.

Intensity was promising because there was no requirement of a threshold. We simply outlined the profile of the powder from subtracted images and calculated the mean gray value of it. As explained in the introduction section of the Methodology, intensity refers to the sum of all the gray pixels in a selected area. Therefore, increasing powder should have increased the sum of gray pixels in the selected area, which is the part profile. We found that this was corroborated in our experiments because increasing powder layer thickness led to increasing intensity.

Because we had over a thousand images to analyze from our camera repeatability test, we wanted to find a more efficient way of calculating intensity of each part without going through an individual manual selection for each. This is when we learned how to create macros in ImageJ. We used the command recorder function to trace each part using the polygon selection tool and produce the intensity measurement after each profile trace. This was saved as a text file and we were then able to run this macro on every image from the camera repeatability test. We then used the macro to find the intensity value for every part in each layer tested.

Chapter 6: Results and Discussion

6.1. Boundary Layer Thickness Significance Test at 90% confidence

We first wanted to check whether the onboard camera could distinguish between layers that were only 0.25 units apart. We especially wanted to check this at the lowest and highest values of the thickness specification range as well as at the layers with thicknesses 0.25 units above and 0.25 units below those limit values. This is because if a part has a 0.5 unit layer of powder, it is out of the specification, but if it has 0.75 unit of powder, it is within specification. We first consolidated all the intensity values and labeled them by part, since each part had distinct intensity values. Each setup was considered a replicate.

It would have been preferable to have at least 10 replicates per layer, but we could not use certain replicates because of powder defects that made the intensity values lack credibility. It also would have been optimal to have gotten replicates with the same standard operating procedure. As discussed previously, the procedure for the camera repeatability test underwent several revisions, as we made improvements after every few tests. Due to time constraints, we could not get an adequate amount of replicates that all used the most improved procedure.

After consolidating intensity values, we first plotted the replicates for each layer within its own setup for layers that had over 5 replicates. We only considered layers with over 5 usable replicates because fewer replicates would make it harder to distinguish between random variability and a real deviation from the norm. We plotted the replicates on a normal probability plot to see if the values all centered strongly around one value or if they were more spread out.

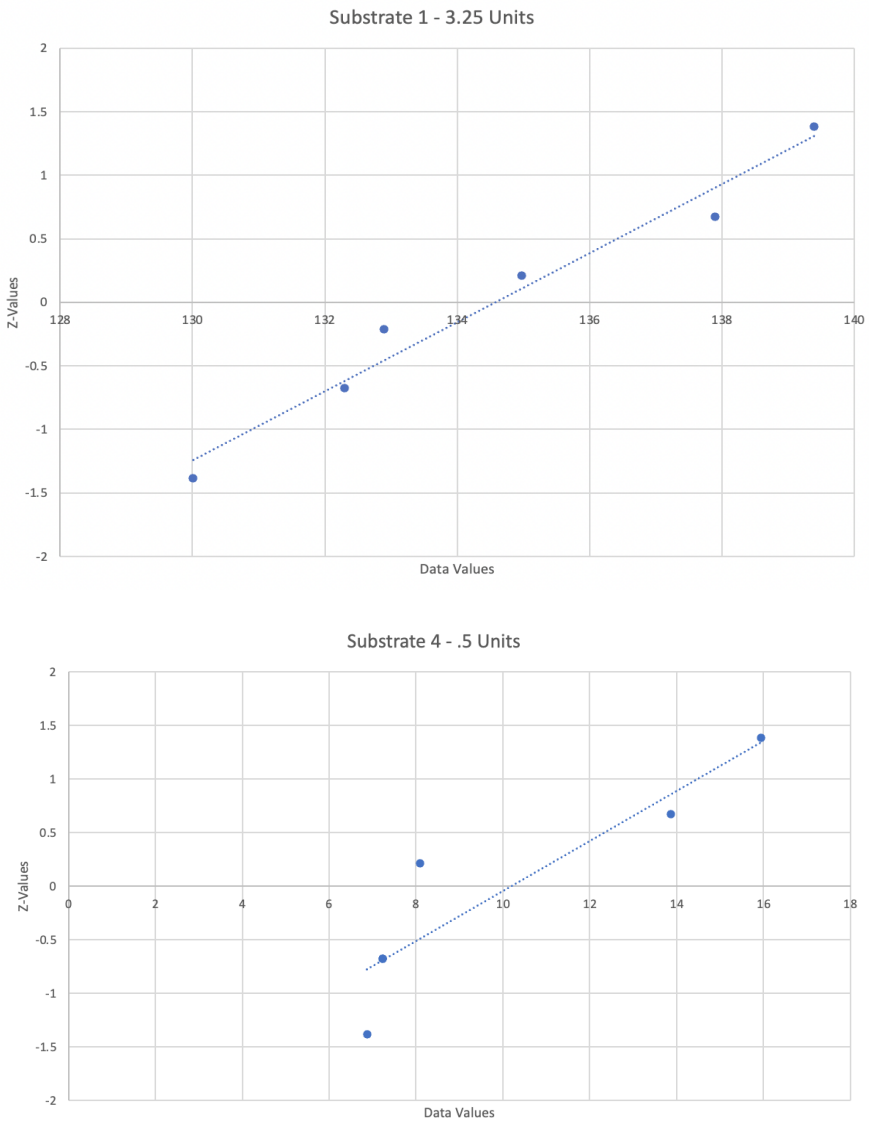

Figure 5. The above graphs are typical normal probability plots of the layers from the camera repeatability test with over 5 replicates. The upper plot shows normally distributed data (seen for 5 out of the 14 tests) and the lower shows non-normal behavior typical of the other tests.

As shown above, some graphs had linear plots at approximately a 45° angle, indicating the replicates fall on a normal distribution. Other graphs, however, showed that the replicates are spread farther apart. This indicates that the layer may not be repeatable across different setups. However, repeatability of the same layer was not as much of a concern to us, since we mainly wanted to see if

the onboard camera can distinguish between different layer thicknesses. Still, these results were important to keep in mind. It would be recommended to have many more replicates per layer, all acquired by following a consistent procedure, to conclude with more credibility whether they follow a normal distribution.

We then performed an analysis of variance (ANOVA) to see if the difference between mean intensity values between two successive layers, 0.25 units apart, at and around the specification boundary values was significant. We performed single factor ANOVA in Excel for 0.5 units to 0.75 units, 0.75 units to 1 unit, 2.75 units to 3 units, 3 units to 3.25 units, and 3.25 units to 3.5 units. Setting the confidence level at 90%, we found that the difference between mean intensity values was significant for 55 out of 60 data points. For the points that were insignificant, the highest p-value was 0.12, signifying that at 80% confidence all data points would be significant.

Table 2. The table below demonstrates which successive layers produced a significant p-value in the ANOVA at a 90% confidence level.

Do the difference between mean intensity values in the below layers show significance at 90% confidence?					
	.5 | .75	.75 | 1	2.75 |3	3 | 3.25	3.25 | 3.5
Metal Substrate 1	**Significant**	**Significant**	**Insignificant (~87%)**	**Significant**	**Significant**
Metal Substrate 2	**Significant**	**Significant**	**Significant**	**Insignificant (~88%)**	**Significant**
Metal Substrate 3	**Significant**	**Significant**	**Significant**	**Significant**	**Significant**
Metal Substrate 4	**Significant**	**Significant**	**Significant**	**Significant**	**Significant**

6.1.1. Discussion

There were a few issues that weakened the above analysis. For the first two setups, the recoater blade was not replaced after each setup, which led to an increased amount of powder defects and anomalies. We started replacing the recoater blade after each setup starting with the third replicate. We learned how to produce more ideal results after the first two setups and made the above

changes as a result. If not for time constraints, it would have been most desirable to analyze intensity values after implementing all improvements, to have the most accurate and consistent results. It is likely that the inconsistency in procedures between setups led to some of them demonstrating normal behavior among replicates and others not. Moreover, since the first two setups resulted in an increased amount of powder defects and anomalies, it is most likely that these issues led to non-normal behavior. Additionally, one issue we found with our data after beginning analysis was that within a part for a single layer, there were often not enough data points to graph all the replicates for every layer normal distribution plot to see whether the points are centered closely around one value or broadly scattered. This would be the first step in future analysis once there are more replicates.

However, from the data we collected and analysis we performed, we saw consistently that intensity increased with powder thickness. We also identified from the significance test that there was a significant difference between 91.66% of mean intensity values between successive layers at the important boundary values at 90% confidence. This provided us sufficient evidence that the onboard camera could successfully distinguish between .25 units, at least based on intensity. With these results and insights, we moved to the next step of correlating the output from the current process check on each part to intensity.

6.2. Correlating the Current Process Check to Intensity Values

For each layer within a setup, we used the current process check to examine all parts and determine which would pass the requirements to start a build. There are various criteria to pass a part including being devoid of any powder anomalies or defects. Additionally, the powder layer could not be too thin or too thick. An example of the data for the current process check for a single setup is demonstrated in Table 3.

Table 3. Data for the current process check is shown below. “B” is for bad and “G” is for good; if a cell is marked as “B,” this means the part’s powder layer would not pass the current criteria for having an in-specification layer. A “G” would mean it does. The top, orange-colored row indicates the setup number (i.e. S1 is setup 1) and the layer thickness (i.e. L1.25 is a 1.25 unit layer).

	S1L10	S1L20	S1L30	S1L40	S1L50	S1L60	S1L70	S1L80	S1L90	S1L100
P1	B	B	B	B	B	G	G	G	G	G
P2	G	G	G	G	G	G	G	G	G	G
P3	G	G	G	G	G	G	G	G	G	G
P4	B	G	G	G	G	G	G	G	G	G
	S1L110	S1L120	S1L130	S1L140	S1L150	S1L160	S1L170	S1L180	S1L190	S1L200
P1	B	B	B	B	B	B	B	B	B	B
P2	G	B	B	B	B	B	B	B	B	B
P3	G	B	B	B	B	B	B	B	B	B
P4	G	B	B	B	B	B	B	B	B	B

As described previously, the intensity was found using the subtraction method and macro tool in ImageJ. As can be seen in the yellow-highlighted rows below, followed a pattern of “bad-good-bad,” which translated broadly to the powder layer being too thin to appear within specification to be too thick.

Table 4. The row highlighted below shows where the layer goes from bad, or out of specification according to the current process check, to in the specification, out of specification once again. The data is the same as that in table 3.

	S1L10	S1L20	S1L30	S1L40	S1L50	S1L60	S1L70	S1L80	S1L90	S1L100
P1	B	B	B	B	B	G	G	G	G	G
P2	G	G	G	G	G	G	G	G	G	G
P3	G	G	G	G	G	G	G	G	G	G
P4	B	G	G	G	G	G	G	G	G	G
	S1L110	S1L120	S1L130	S1L140	S1L150	S1L160	S1L170	S1L180	S1L190	S1L200
P1	B	B	B	B	B	B	B	B	B	B
P2	G	B	B	B	B	B	B	B	B	B
P3	G	B	B	B	B	B	B	B	B	B
P4	G	B	B	B	B	B	B	B	B	B

This pattern of “bad-good-bad” enabled the creation of intensity limits. The end objective was that a user could take an image of the build plates with the onboard camera and an automated macro could be installed to go through the steps of extracting the intensity values using ImageJ. Within this macro, each computed intensity value would be compared to the set intensity limits. If

the intensity value for each part was within the corresponding set intensity limits, the user would be notified that these parts can pass to start a build. If the values are outside the set intensity limits, the user would be notified of this and whether it is because the layer is too thin or too thick.

We then went to the next set of current process check data and found where the "bad-good-bad" pattern occurred for part 4 in a different setup. Overall, 6 total records of process checks were used. Using all "bad-good-bad" corresponding intensity values, we set intensity limits that would broadly encompass all the "good" layers for part 4. Table 5 shows how the analysis was done. The green boxes labeled 0.25 units to 5 units represent the layer thicknesses, while each row corresponds to a different setup. The boxes marked red were considered "bad" by the current process check, while those marked green were considered "good."

Table 5. The table below demonstrates the intensity values at the bad to good and good to bad thresholds for part 4.

		0.25	0.5	0.75	1	1.25	1.5	1.75	2	2.25	2.5
P4	7/19/22	43.239	45.946								
	7/19/22										
	7/19/22							42.885	75.138		
	7/12/22				30.226	38.746					
	7/12/22									88.189	103.786
	7/12/22										
		2.75	3	3.25	3.5	3.75	4	4.25	4.5	4.75	5
	7/19/22	157.947	190.039								
	7/19/22	134.731	155.001								
	7/19/22		170.35	172.541							
	7/12/22						193.016	196.119			
	7/12/22						173.146	194.195			
	7/12/22								82.44	107.572	
	Limits Recommendations	95-150									

We did the same process for all parts. The final intensity limits are shown below in Table 6.

6.2.1 Discussion

Like the significance test, credibility for the intensity limits would have been greater if we had even more current process check data. However, for this test, the process check itself contributed some variability to the data due to the nature of the test which cannot be discussed in detail here. But the process check, despite being based on a certain set of criteria, is ultimately subjective. So, there is likely some variation attributed to the process check.

Overall, the results indicated a fair amount of consistency between intensity values for the same layer across different setups. Also, despite external conditions affecting intensity values, we were still able to establish broad ranges for intensity limits, so that the characterization process would not be too hindered by the implementation of these limits.

The details of how each step the Excel macro works is explained in Satvik Sabarad's thesis [74]. The mean intensity-based macro predicted 31 test images correctly out of a total of 34, which gave an accuracy rate of 91%. With more test images, this accuracy rate and the intensity limits per part can become further refined.

Chapter 7: Conclusion

We found that the onboard camera was able to tell the difference between successive layers 0.25 units apart through intensity values. As explained above, this was found by performing a significance test and finding that over 90% of the difference between mean intensities from one layer to the next was significant. While this is promising, there was not an equal amount of replicates for every layer. If there were at least 10 replicates for every layer, this would have refined the variance for each layer and would have provided more credibility to the analysis. We ended up doing over 10 replicates for each layer from all our camera repeatability tests. However, many could not be considered because of powder defects and issues with the build plate and recoater blade. So, we could only consider the replicates that had successful setups and conditions and therefore suitable intensity values. With a now refined procedure for performing the camera repeatability tests, given more time, we would have been able to create more replicates for improved analysis. This may have also helped us to increase the confidence level for all data to 95% or above, which is ideal.

We were able to establish intensity limits based on the current process check data that can be used to automatically tell users if a layer is in the specification or not.. This was done by attempting to correlate intensity values to the MicroEpsilon sensor readings. This will be further explained in Satvik Sabarad's thesis [74]. The implementation of an automated approach based on intensity values would allow for an objective and efficient solution to characterize the characterization.

7.1. Future Work

For the future, it would be important to take and analyze data from setups that employ consistent procedures throughout.While this requires a lot of time, it will ensure that there will be no variation in data attributable to factors like lack wear of the recoater blade, and differing biases from

the current process check. In the future it would also be important to have many more replicates, at least 10, per layer to refine the variances for the significance tests and increase the confidence level. This would also help in refining the intensity limits that have been set. Additionally, with this many replicates, the behavior of the replicates, namely if they follow a normal distribution, could be elucidated.

7.2. Recommendations

It would be recommended to look further into the onboard camera. Additionally, future teams could look into other cameras that provide even higher resolution so that values like intensity are even more accurate and values like percentage area coverage could be considered. Once the solution is ready to be deployed, step-by-step guidelines for how to use the macro should be recorded for users to follow.

7.3. Overall Project Conclusion

The overall goal of the project was to quantify an important powder layer characteristic and create a verification tool that a user could use to check the quality of their characterization set up before they start a build. The aim of the project was to use the existing sensors and cameras available on an AM machine to perform this check. The performance of other available cameras was studied in Modes' thesis. The results show that the onboard camera yielded the most repeatable and reproducible results. Modes' thesis also found that results from onboard camera captured images and video snapshots yield the same results, so captured images can be used moving forward [72].

The Micro-Epsilon laser line scanner showed promise over the confocal chromatic sensor in providing powder thickness and percent coverage data for correlation. Percent coverage seemed to

be a more distinguishable metric, though the process used ended up not being precise enough to come to a firm conclusion about the results. The correlation is not possible with the setup and data alignment methods used [73]. Improvements to the testing equipment including development of a micron-scale repeatable mount and precision stage will improve the results. Moving forward with the current process check output for layer distinction is still a viable option for layer characterization since this is the current method being used.

From our analysis of the onboard camera, we found that it could determine the difference between mean intensity values of layers only 0.25 units apart at a 90% confidence level. We were also able to establish a broad range of intensity limits that were detailed in the results sections of this thesis. If there were more replicates from the camera repeatability test, and if each replicate was performed using a consistent procedure, the variance would have been refined for each layer and would have provided more credibility to the analysis. Also, we could have possibly increased the confidence level of the significance test.

Exploring the onboard camera gave promising results on distinguishing between “too thin,” “acceptable,” and “too thick” layers. Gauge Repeatability and Reproducibility (GR&R) proved that the results were repeatable across different setups. Improvements must be made in the laser triangulation sensor to establish a strong correlation between the ground truth values and camera intensity values. A machine-user interface was developed which could help a user in making decisions on “acceptable” layers. The second method, (Convolutional Neural Network (CNN) based machine learning model), classified the images into “too thin,” “acceptable,” and “too thick” categories with 94% accuracy. All of these results are detailed in Satvik Sabarad’s thesis [74].

References

[1] *Optimising Performance and Manufacturability for Additive Manufacturing | ManufacturingTomorrow*. https://manufacturingtomorrow.com/article/2020/03/optimising-performance-and-manufacturability-for-additive-manufacturing/15026. Accessed 1 Aug. 2022.

[2] S. S. Babu, L. Love, R. Dehoff, W. Peter, T. R. Watkins, and S. Pannala, "Additive Manufacturing of materials: Opportunities and challenges," *MRS Bulletin*, vol. 40, no. 12, pp. 1154–1161, 2015.

[3] R. McCann *et al.*, "In-situ sensing, process monitoring and machine control in Laser Powder Bed Fusion: A review," *Additive Manufacturing*, vol. 45, p. 102058, Sep. 2021, doi: 10.1016/j.addma.2021.102058.

[4] M. S. Hossain and H. Taheri, "In situ process monitoring for additive manufacturing through acoustic techniques," *Journal of Materials Engineering and Performance*, vol. 29, no. 10, pp. 6249–6262, 2020.

[5] M. Saleem and G. Krammer, "Optical in-situ measurement of filter cake height during bag filter plant operation - ScienceDirect," *Science Direct*. https://www.sciencedirect.com/science/article/pii/S0032591006005468 (accessed Jun. 28, 2022).

[6] B. Lane, L. Jacquemetton, M. Piltch, and D. Beckett, "Thermal calibration of commercial melt pool monitoring sensors on a laser powder bed fusion system," 2020.

[7] "Machine Learning: A Game Changer for Additive Manufacturing Quality," *Sigma Additive Solutions*. https://sigmaadditive.com/machine-learning-a-game-changer-for-additive-manufacturing-quality-assurance/ (accessed Jun. 15, 2022).

[8] R. Frye, C. Xuan Yu, S. Betts, and L. Jacquemetton, “Data Registration and Machine Learning for Anomaly Detection,” *Sigma Labs Technical Paper*, pp. 1–8,Oct. 2019.

[9] L. Jacquemetton and S. Betts, “PrintRite3D Alerts for Anomaly Detection,” *Sigma Labs Technical Paper*, pp. 1–10, Oct. 2019.

[10] “Resolving Power of the Eye.” https://stokes.byu.edu/teaching_resources/resolve.html (accessed Jul. 08, 2022).

[11] “QM Coating - Concentration monitoring system by Concept Laser | DirectIndustry.” https://www.directindustry.com/prod/concept-laser/product-15662-1827567.html (accessed Jun. 29, 2022).

[12] C. Burgess, “OPTICAL SPECTROSCOPY | Radiation Sources,” in *Encyclopedia of Analytical Science (Second Edition)*, P. Worsfold, A. Townshend, and C. Poole, Eds. Oxford: Elsevier, 2005, pp. 427–431. doi: 10.1016/B0-12-369397-7/00429-5.

[13] A. Cosentino, “Practical notes on ultraviolet technical photography for art examination,” *Cultural Heritage Science Open Source*. Online: https://chsopensource.org/download-practical-notes-on-ultraviolet-technical-photography-for-art-examination/ (accessed Jun. 14, 2022)

[14] “Lidar - A measurement technique that uses light emitted from a sensor to measure the range to a target object. · VectorNav.” https://www.vectornav.com/applications/lidar-mapping (accessed Jun. 15, 2022).

[15] A. Thompson, I. Maskery, and R. K. Leach, “X-ray computed tomography for additive manufacturing: a review,” *Meas. Sci. Technol.*, vol. 27, no. 7, p. 072001, Jun. 2016, doi: 10.1088/0957-0233/27/7/072001.

[16] M. S. Xavier, S. Yang, C. Comte, A. Bab-Hadiashar, N. Wilson, and I. Cole, “Nondestructive quantitative characterisation of material phases in additive manufacturing using multi-energy synchrotron X-rays microtomography,” *Int J Adv Manuf Technol*, vol. 106, no. 5, pp. 1601–1615, Jan. 2020, doi: 10.1007/s00170-019-04597-y.

[17] J.R. Fowler and A. M. Ilyas, “The Accuracy of Digital Radiography in Orthopaedic Applications,” *Clin Orthop Relat Res*, vol. 469, no. 6, pp. 1781–1784, Jun. 2011, doi: 10.1007/s11999-010-1628-6.

[18] “X-ray - NHS.” https://www.nhs.uk/conditions/x-ray/ (accessed Jul. 09, 2022).

[19] “What is lidar? Learn How Lidar Works,” *Velodyne Lidar*. https://velodynelidar.com/what-is-lidar/ (accessed Jun. 15, 2022).

[20] “Lidar - A measurement technique that uses light emitted from a sensor to measure the range to a target object. VectorNav.” https://www.vectornav.com/applications/lidar-mapping (accessed Jun. 15, 2022).

[21] "NIR Technology. ThermoFisher Scientific." https://www.thermofisher.com/us/en/home/industrial/spectroscopy-elemental-isotope-analysis/spectroscopy-elemental-isotope-analysis-learning-center/molecular-spectroscopy-information/nir-technology.html (accessed Jun. 10, 2022).

[22] M.-E. M.- info@micro-epsilon.de, "Laser triangulation | Micro-Epsilon," *Micro-Epsilon Messtechnik*. https://www.micro-epsilon.com (accessed Jun. 30, 2022).

[23] "Laser scanners for 2D/3D profile measurement | Micro-Epsilon Optronic GmbH." https://www.micro-optronic.com/technology/Laser-Profil-Scanner/ (accessed Jun. 30, 2022).

[24] B. Smith, "A Comparison of Optical Methods Used for Topography," AZoM.com, Feb. 01, 2019. https://www.azom.com/article.aspx?ArticleID=17573 (accessed Jul. 07, 2022).

[25] A. Townsend, L. Pagani, P. Scott, and L. Blunt, "Areal surface texture data extraction from X-ray computed tomography reconstructions of additively manufactured parts," *Precision Engineering*, vol. 48, pp. 254–264, Apr. 2017, doi: 10.1016/j.precisioneng.2016.12.008.

[26] "CCS Prima Confocal Displacement Sensor," Acuity Laser. https://www.acuitylaser.com/product/laser-sensors/confocal-sensors/ccs-prima-confocal-displacement-sensor/ (accessed Jun. 19, 2022).

[27] Z. Li *et al.*, "In Situ 3D Monitoring of Geometric Signatures in the Powder-Bed-Fusion Additive Manufacturing Process via Vision Sensing Methods," *Sensors*, vol. 18, no. 4, Art. no. 4, Apr. 2018, doi: 10.3390/s18041180.

[28] J. C. A. Read, "Stereo vision and strabismus," Eye, vol. 29, no. 2, pp. 214–224, Feb. 2015, doi: 10.1038/eye.2014.279.

[29] Z. Yaqoob, J. Wu, and C. Yang, "Spectral domain optical coherence tomography: a better OCT imaging strategy," *BioTechniques*, vol. 39, no. 6S, pp. S6–S13, Dec. 2005, doi: 10.2144/000112090.

[30] A. Neef, V. Seyda, D. Herzog, C. Emmelmann, M. Schönleber, and M. Kogel-Hollacher, "Low Coherence Interferometry in Selective Laser Melting," *Physics Procedia*, vol. 56, pp. 82–89, Jan. 2014, doi: 10.1016/j.phpro.2014.08.100.

[31] J. A. Kanko, A. P. Sibley, and J. M. Fraser, "In situ morphology-based defect detection of selective laser melting through inline coherent imaging," *Journal of Materials Processing Technology*, vol. 231, pp. 488–500, May 2016, doi: 10.1016/j.jmatprotec.2015.12.024.

[32] P. J. DePond *et al.*, “In situ measurements of layer roughness during laser powder bed fusion additive manufacturing using low coherence scanning interferometry,” *Materials & Design*, vol. 154, pp. 347–359, Sep. 2018, doi: 10.1016/j.matdes.2018.05.050.

[33] “Thermal sensors: Characteristics and applications,” *Lynred.com*. [Online]. Available: https://lynred.com/blog/thermal-sensors-characteristics-and-applications. [Accessed: 15-Jun-2022].

[34] “Hints for Selecting the Correct Temperature Sensor for Your Application,” www.agilent.com, 16-Apr-2008. [Online]. Available: https://www.newark.com/wcsstore/ExtendedSitesCatalogAssetStore/cms/asset/images/americas/common/mro/on_demand/nov2013/Hints-for-Selecting-the-Correct-Temperature-Sensor-for-Your-Application.pdf. [Accessed: 11-Jun-2022].

[35] How to Get Great Results with an Infrared Thermometer. https://www.fluke.com/en-us/learn/blog/temperature/how-to-get-great-results-with-an-infrared-thermometer. Accessed 15 June 2022.

[36] MoviTHERM, “What is flash thermography?,” MoviTHERM, 08-Jul-2022. [Online]. Available: https://movitherm.com/knowledgebase/what-is-flash-thermography/. [Accessed: 15-Jun-2022].

[37] H. Rieder, M. Spies, J. Bamberg, and B. Henkel, “On- and offline ultrasonic characterization of components built by SLM additive manufacturing,” Minneapolis, Minnesota, 2016, p. 130002. doi: 10.1063/1.4940605.

[38] W. Nan, M. Pasha, T. Bonakdar, A. Lopez, and U. Zafar, “Jamming during particle spreading in additive manufacturing,” *Powder Technology*, vol. 338, pp. 253–362, Oct. 2018, doi: https://doi.org/10.1016/j.powtec.2018.07.030.

[39] A. Phua, P. S. Cook, C. H. J. Davies, and G. W. Delaney, “Powder spreading over realistic laser melted surfaces in additive manufacturing,” *Additive Manufacturing Letters*, vol. 3, p. 100039, Dec. 2022, doi: 10.1016/j.addlet.2022.100039.

[40] F. Rosala, Improvement and Development of Powder Spreadability Testing. 2021. Accessed: Jul. 27, 2022. [Online]. Available: http://urn.kb.se/resolve?urn=urn:nbn:se:kth:diva-301259

[41] “Standard terminology of Powder,” *ASTM International - Standards Worldwide*. [Online]. Available: https://www.astm.org/b0243-22.html. [Accessed: 31-Jul-2022].

[42] M. Mitterlehner, H. Gschiel, H. Danninger, and C. Gierl-Mayer, “Investigation of the Impact of Powder Shape on Spreading Dense Layers Using the Spreading Tester,” *Berg Huettenmaenn Monatsh*, vol. 167, no. 7, pp. 300–307, Jul. 2022, doi: 10.1007/s00501-022-01243-1.

[43] R. P. Behringer, “Jamming in granular materials,” *Comptes Rendus Physique*, vol. 16, no. 1, pp. 10–25, 2015.

[44] T. Craeghs, S. Clijsters, and E. Yasa, “Online Quality Control of Selective Laser Melting,” *University of Texas Libraries*, Jun. 2011, [Online]. Available: https://repositories.lib.utexas.edu/handle/2152/88350

[45] L. Scime, D. Siddel, S. Baird, and V. Paquit, “Layer-wise anomaly detection and classification for Powder Bed Additive Manufacturing Processes: A machine-agnostic algorithm for real-time pixel-wise semantic segmentation,” *Additive Manufacturing*, vol. 36, p. 101453, 2020.

[46] F. Caltanissetta, M. Grasso, S. Petrò, and B. M. Colosimo, “Characterization of in-situ measurements based on layerwise imaging in Laser Powder Bed Fusion,” *Additive Manufacturing*, vol. 24, pp. 183–199, 2018.

[47] T. Furumoto, “Experimental investigation of melt pool behaviour during selective laser melting by high speed imaging,” *CRP Annals - Manufacturing Technology*,” May 2018. [Online]. Available: https://www.researchgate.net/publication/324915801_Experimental_investigation_of_melt_pool_behaviour_during_selective_laser_melting_by_high_speed_imaging (accessed June 15, 2022).

[48] M. Abdelrahman, E. W. Reutzel, A. R. Nassar, and T. L. Starr, “Flaw detection in powder bed fusion using optical imaging,” *Additive Manufacturing*, vol. 15, pp. 1–11, 2017.

[49] F. G. Fischer, N. Birk, L. Rooney, L. Jauer, and J. H. Schleifenbaum, “Optical process monitoring in laser powder bed fusion using a recoater-based line camera,” *Additive Manufacturing*, vol. 47, p. 102218, 2021.

[50] W. Lin, D. A. Gonçalves, A. de Pereira, M. Pereira, and W. L. Weingaertner, “Quality Analysis Method for powder deposited layers applicable to selective laser sintering and selective laser melting processes,” *Journal of Laser Applications*, vol. 31, no. 2, p. 022306, 2019.

[51] T. Kumar and K. Verma, “A theory based on conversion of RGB image to Gray Image,” *International Journal of Computer Applications*, vol. 7, no. 2, pp. 5–12, 2010.

[52] “How are images stored on a computer: Grayscale & RGB image formats,” *Analytics Vidhya*, 18-Mar-2021. [Online]. Available:

https://www.analyticsvidhya.com/blog/2021/03/grayscale-and-rgb-format-for-storing-images/. [Accessed: 31-Jul-2022].

[53] F. Hunter, S. Biver, P. Fuqua, and R. Reid, Light - science and magic an introduction to photographic lighting. New York: Routledge, 2021.

[54] bjorn@acuitylaser.com, "Laser Triangulation Sensors - Non-Contact Measurement," *Acuity Laser*. https://www.acuitylaser.com/sensor-resources/laser-triangulation-sensors/ (accessed Jul. 08, 2022).

[55] F. Froment, "An Introduction to Laser Triangulation Sensors," *Third Dimension*, Apr. 08, 2021. https://www.third.com/an-introduction-to-laser-triangulation-sensors/ (accessed Jul. 08, 2022).

[56] S. Donadello, M. Motta, A. G. Demir, and B. Previtali, "Monitoring of laser deposition height by means of coaxial laser triangulation," *Optics and Lasers in Engineering*, vol. 112, pp. 136–144, Jan. 2019, doi: 10.1016/j.optlaseng.2018.09.012.

[57] M. Erler, A. Streek, C. Schulze, and H. Exner, "Novel Machine and Measurement Concept for Micro Machining by Selective Laser Sintering," 2014. doi: 10.26153/tsw/15660.

[58] "What is Laser Triangulation," *MoviMed.* https://www.movimed.com/knowledgebase/what-is-laser-triangulation/ (accessed Jul. 08, 2022).

[59] F. Aquino, W. M. Jadwisienczak, and F. Rahman, "Effect of laser speckle on light from laser diode-pumped phosphor-converted light sources," *Appl. Opt., AO*, vol. 56, no. 2, pp. 278–283, Jan. 2017, doi: 10.1364/AO.56.000278.

[60] "What is Structured Light Imaging? | RoboticsTomorrow." https://roboticstomorrow.com/article/2018/04/what-is-structured-light-imaging/11821 (accessed Jul. 07, 2022).

[61] B. Zhang, J. Ziegert, F. Farahi, and A. Davies, "In situ surface topography of laser powder bed fusion using fringe projection," *Additive Manufacturing*, vol. 12, pp. 100–107, Oct. 2016, doi: 10.1016/j.addma.2016.08.001.

[62] A. D. Elliott, "Confocal Microscopy: Principles and Modern Practices," Curr Protoc Cytom, vol. 92, no. 1, p. e68, Mar. 2020, doi: 10.1002/cpcy.68.

[63] J. Elambasseril, J. Rogers, C. Wallbrink, D. Munk, M. Leary, and M. Qian, "Critical Reviews in Solid State and Materials Sciences," vol. 0, no. 0, pp. 1–37, Mar. 2022, doi: 10.1080/10408436.2022.2041396.

[64] "Technical Explanation for Displacement Sensors and Measurement Sensors," OMRON. https://www.ia.omron.com/support/guide/56/introduction.html (accessed Jun. 21, 2022).

[65] C. Jones, "Factors to consider when selecting confocal displacement sensors," Eureka, Jun. 05, 2018. https://www.eurekamagazine.co.uk/content/technology/factors-to-consider-when-selecting-confocal-displacement-sensors/ (accessed Jun. 20, 2022).

[66] Keyence, Confocal Displacement Sensor CL-3000 Series.

[67] Y. Yang, "CONFOCAL SCANNING IMAGING SYSTEM FOR SURFACE CHARACTERIZATION IN ADDITIVE MANUFACTURING SYSTEM," p. 79, Dec. 2019, [Online]. Available: https://etd.ohiolink.edu/apexprod/rws_etd/send_file/send?accession=dayton1576066631705912&disposition=inline

[68] J. Modes, "Optical In-Process Monitoring Tools for Laser Powder Bed Fusion: Verifying Powder Area Coverage of an Initial Layer Setup," thesis, 2022.

[69] J. Wittenbrink, "Using Displacement Sensors to Characterize Critical Powder Layers in Laser Powder Bed Fusion," thesis, 2022.

[70] S. Sabarad, "Correlating Displacement Sensors and In-Situ Optical Imaging for the Initial Layer Setup in a Laser Powder Bed Fusion Process," thesis, 2022.

[71] "Analyze Menu," ImageJ, National Institutes of Health. https://ImageJ.nih.gov/ij/docs/menus/analyze.html (accessed Jun. 29, 2022).

[72] D. Bhatt, A comprehensive guide for Camera calibration in computer vision," Oct. 30, 2021. [Online] Available: https://www.analyticsvidhya.com/blog/2021/10/a-comprehensive-guide-for-camera-calibration-in-computer-vision/.